International Journal of Engineering Trends and Technology
ISSN: 2231 – 5381 / https://doi.org/10.14445/22315381/IJETT-V70I11P203

Volume 70 Issue 11, 19-27, November 2022

Original Article

Image Denoising using Adaptive Patch Clustering with Suboptimal Wiener Filter in PCA Domain

Swati Rane[1], Lakshmappa Ragha[2], Siddalingappagouda Biradar[3], Vaibhav Pandit[4]

[1]*Department Electronics and Telecommunication Engineering, SIES Graduate School of Technology, University of Mumbai, Maharashtra, India*
[2, 4]*Department Electronics and Telecommunication Engineering, Terna Engineering College, University of Mumbai, Maharashtra, India*
[3]*Department of Electronics & Communication Engineering, Dayananda Sagar Academy of Technology & Management, Visvesvarya Technological University, Karnataka, India*

[1]*Corresponding Author: swati.rane@siesgst.ac.in*

Received: 14 July 2022 Revised: 31 October 2022 Accepted: 05 November 2022 Published: 26 November 2022

Abstract *- The degradation in the visual quality of images is often seen due to various noises added inevitably at the time of image acquisition. Its restoration has thus become a fundamental and significant problem in image processing. Many attempts have been made in the recent past to efficiently denoise such images. But, the best possible solution to this problem is still an open research problem. This paper validates the effectiveness of one such popular image denoising approach, where an adaptive image patch clustering is followed by the suboptimal Wiener filter operation in the Principal Component Analysis (PCA) domain. The experimentation is conducted on grayscale images corrupted by four different noise types: speckle, salt & pepper, Gaussian, and Poisson. The efficiency of image denoising is quantified in terms of various famous image quality metrics. The comprehensive performance analysis of the denoising approach against the four noise models underlies its suitability for various applications. It certainly gives the new researchers a direction for selecting the image-denoising method.*

Keywords *- Adaptive clustering, Image denoising, Principal component analysis, Wiener filter.*

1. Introduction

Denoising of noise-corrupted images is a very significant step in many image processing problems like image registration [1], image segmentation [2], image classification [3], etc., where the performance mainly depends on the correctness of original image contents. In short, image denoising improves a raw image's quality and creates a good foundation for its subsequent processing. Today, massive production of digital images is often undertaken in non-ideal image acquisition conditions. It certainly needs efficient image denoising to retain the visual quality contents of an image for the end use [4]. In the past few years, many image-denoising methodologies have been developed. Many methods use one or the other type of filter like linear, non-linear, local, global, simple, adaptive, etc.

The image-denoising techniques can be categorized as pixel-based and patch-based. The extensive use of patch-based methods [5] is observed in the image-denoising domain. These methods are based on the fact that similar regions or patches are present in images mostly locally. These methods divide the noisy image into overlapping or non-overlapping patches. Similar regions or patches are present in images, mostly locally. These methods divide the noisy image into overlapping or non-overlapping patches. Then these patches are processed individually, and an estimate of the ground truth is obtained using the similarity between various patches of the input image.

Patch-based methods result in promising estimates of noise-free images and smooth flat regions. They can also maintain image features like sharp edges and fine details. However, these methods are quite time-consuming, including grouping and comparing similar patches. Secondly, patch-based methods make use of a large number of parameters that are simultaneously very difficult to adjust correctly. However, patch-based methods are still preferred because of their significant advantages, like good noise suppression. However, simultaneously, these methods have some limitations, resulting in loss of information or alteration of original contents. This paper validates the effectiveness of one such popular image-denoising approach in which the suboptimal Wiener filter follows an adaptive patch clustering in the PCA domain to remove the noise from the image corrupted with four types of noises. The effectiveness is measured using the peak signal-to-noise ratio (PSNR), structural similarity (SSIM), feature similarity (FSIM), and denoising time, and their comparative analysis is presented.

The outline of the remaining paper is Section 2 briefs the related work. The methodology of the various adaptive approach for image denoising is presented in Section 3. Experimentation of applying denoising algorithms on images and its result analysis is addressed in Section 4. Lastly, Section 5 concludes the complete paper.

2. Related Work

Researchers have proposed several methods to eliminate various types of noises in the images used in various applications. Some techniques use filters for noise removal [6], [7]. Some include patch-based and block-based image-denoising algorithms presented in [8]. One such method is Block-matching and 3D filtering (BM3D) [9], which has two steps: a hard-thresholding and a Wiener filter stage. Both involve 3D block transformation, grouping, collaborative filtering, and aggregation. BM3D is an efficient and fast algorithm that results in the perfect preservation of structuring details with only a few muddling artifacts comparatively for high noise levels. A further improvement in the BM3D algorithm is proposed by Yahya et al. in [10], in which the hard thresholding is replaced by adaptive thresholding as per noise contents in local regions. Nevertheless, this work has the limitation of computational complexity. Gao and Wang [11] proposed using K-means clustering with BM3D, which helped to lessen the computational burden of the algorithm.

One more efficient image denoising method is using PCA with local pixel grouping (LPG), which is good at preserving local structures in an image [12], [13] and effectively eliminating small artifacts [14]. Muresan and Parks [15] proposed an adaptive PCA denoising method that adopted linear minimum mean square error (LMMSE) [16] to shorten the length of the total transform coefficients of PCA for noise removal. Some patch-based image-denoising algorithms use Wiener filters [17] that use redundancy present in patches to estimate the filter parameters [18]. In their work, Suresh et al. [19] presented the use of a 2-D FIR Wiener filter guided by the cuckoo search algorithm, which is adaptive in nature and used over multispectral satellite images. Leelavathi and Prakash [20] proposed a three-stage algorithm for speckle noise removal in SAR images, including block-based modified PCA, Hybrid Median Filter, and sharpening filter.

Chatterjee and Milanfar [21], [22] in their work analyzed the limitations of the denoising problem and proposed patch-based locally optimal wiener (PLOW) for images based on a statistical foundation, and it has reached the near-optimal bound. However, the original PLOW is unsuitable for denoising images with high noise levels. Hence, Cao et al. in [23] modified the original PLOW algorithm and called it a median PLOW. In that, the original estimator was replaced by a median estimator. In [33], Ote et al. used the Wiener filter in their proposed kinetics-induced block matching and 5-Dimensional transform domain filtering for denoising, resulting in the best output image quality.

3. Methodology

The overview of the adaptive patch clustering approach using suboptimal wiener filtering in the PCA domain is presented in Figure 1.

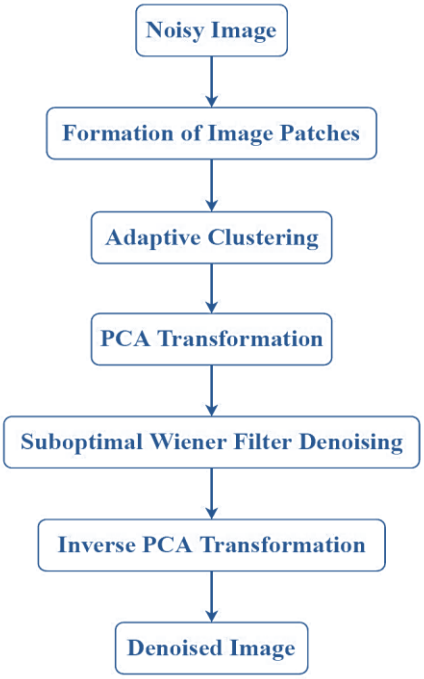

Fig. 1 Methodology

3.1. Noisy Image Model

A noisy image can be mathematically modelled as follows:

$$f_n(x,y) = f(x,y) + \eta(x,y) \quad (1)$$

Where *fn* is noise corrupted image, *x* and *y* represent the corresponding row and column locations of a pixel in an image plane, *f* is the ground truth image, and η is the added noise. This noise can be of any type. Here, the original image is first corrupted by four types of noise models: Gaussian, speckle, salt-and-pepper, and Poisson noise.

3.1.1. Gaussian Noise:

This noise is observed in amplifiers or detectors as an effect of heating the internal components. Gaussian noise model [25] is characterized by its probability density function (PDF) to gray value as:

$$P(r) = \sqrt{\frac{1}{2\pi\sigma^2}}\, e^{\frac{-(r-\mu)^2}{2\sigma^2}} \quad (2)$$

Where *r* is the gray value, μ and σ represent the mean and the standard deviation of gray values, respectively.

3.1.2. Poisson Noise:

This noise occurs because of electromagnetic waves of statistical nature like visible light, x-rays, and gamma rays [25]. This noise exhibits spatial as well as temporal

randomness in the resultant image. The Poisson distribution of grey level r with parameter $\lambda > 0$ has a probability mass function as

$$P(r = k) = \frac{\lambda^k e^{-\lambda}}{k!} \quad (3)$$

Where k represents the number of times r occurs, e represents Euler's number, and λ is the expected value (EV) of r and also its variance.

3.1.3. Speckle Noise:

It is a multiplicative noise usually observed in imaging systems like a laser, radar, and acoustics [26]. Its PDF is given as:

$$P(r) = \frac{r^{\alpha-1} e^{\frac{r}{\alpha}}}{\alpha - 1!\, a^{\alpha}} \quad (4)$$

This noise can be expressed as $f_n = f + \eta * f$, where η is random noise with uniform distribution with mean 0 and variance σ^2.

3.1.4. Salt & Pepper Noise:

It is an impulse type of noise that occurs due to sudden sharp disturbances in the signal [25]. In an image, it can be observed when pixels have either minimum or maximum grey values. The PDF is given by –

$$P(r) = \begin{cases} P_a, & for\ r = a \\ P_b, & for\ r = b \\ 0, & otherwise \end{cases} \quad (5)$$

where *Pa* and *Pb* are the probability with which grey levels a and b are present in the image.

3.2. Image Patch Formation

The noisy image is further processed to form the image patches. The total number of overlapping patches for an image of size $M \times N$ is computed as:

$$Np = (M - p + 1) \times (N - p + 1) \quad (6)$$

Where, p is the size of the patch.

3.3. Adaptive Clustering

All patches are clustered with the K-means clustering algorithm into the *K1* number of clusters.

$$K1 = max\{\frac{MXN}{256\ x\ 256}, 4\} \quad (7)$$

Each of these *K1* clusters is re-clustered once again using the K-means clustering algorithm into the *K2* number of clusters.

$$K2 = \max\{\frac{N_{pi}}{p\ x\ p}, 1\} \quad (8)$$

For each possible pair of clusters, then the cluster distance is computed. These distances are ordered in ascending order. If the distance is less than a threshold *T*, they merge. The process of calculating distances, arranging them in ascending order, and merging is repeated until the minimum cluster distance is larger than the threshold T. Considering any two similar clusters to be merged, the threshold value denotes the most prominent dissimilarity between them, which is acceptable by the user.

3.4. PCA Transformation

Each patch of the noisy image is transmuted into the orthogonal PCA domain. The transform domain signal observation of a noisy image also contains similar noise. The first few principal components show more concentrated total variance than the same noise variance and achieve a higher signal-to-noise ratio. The lowest eigenvalues, which contain the highest noise, are discarded by reducing the dimension of the transform domain signal. For selecting the dimension, the Gaussian spiked population model [27] is used, which suggests that the eigenvalues of noise-dominant dimensions are below λ_{n+} for cluster matrices of normal size. It helps control the trade-off between loss of information and simplification of the problem. $P_R = [p_1, p_2, \ldots, p_R]$ where p_i is the reduced dimension of PCA, and R is the rank of the matrix.

3.5. Suboptimal Wiener Filtering

Before applying the Wiener filter, its parameters are estimated adaptively over a neighborhood of the signal point *p*. If *y(p)* is the signal observation to denoise at point *p*, then the filter parameters to be estimated are its autocovariance $C_y(p)$ and its cross-covariance $C_{fy}(p)$ between *y(p)* and its corresponding noise-free part *f(p)*. A local neighborhood is preferred to select signal patches with high similarity to the signal (at point p) to be estimated. The local polynomial approximation with the intersection of confidence intervals (LPA-ICI) [28] method is used to detect signal variation and select the optimum size of the window adaptively to achieve a balance between bias and variance.

This method assigns the small and large window sizes to the segment with large and small noise variance. For transform domain image noise removal, the Wiener filter [29] performs efficiently when the auto-covariance of the noisy signal at that point and noise auto-covariance are known. The Wiener filter as-estimates the signal f(p) at point p

$$\hat{f}(p) = h_{ow} y(p) \quad (9)$$

where,

$$h_{ow} = C_y(p)^{-1} C_{fy}(n) = [1 - g_{ow}] \quad (10)$$

$$g_{ow} = C_y(p)^{-1} C_w \quad (11)$$

Here $C_y(p)$ is the auto-covariance at point *p*, and $C_w = \sigma^2$ is the auto-covariance of noise. However, signal distortion is often incorporated into the estimated signal during noise

reduction when the optimal Wiener filter is used. A suboptimal Wiener filter helps to bring about a superior balance between the diminution of noise and signal distortion. This suboptimal Wiener filter g_{sw} with an attenuation coefficient α of g_{ow} is obtained by manipulating the Wiener filter as follows:

$$h_{sw} = [1 - \alpha g_{ow}] = [1 - g_{sw}] \quad (12)$$

Where $\alpha \in [0, 1]$ is obtained using signal distortion and noise diminution indices [30], then the suboptimal Wiener filter estimates the signal observation *f(p)* at point *p* as:

$$\hat{f}(p) = h_{sw} y(p) \quad (13)$$

The signal-distortion index used to determine α can be defined as:

$$i_{sd}(g_{sw}) \triangleq \frac{E\{[f(p) - h_s f(p)^2\}}{\sigma_f^2} \quad (14)$$

The noise reduction index or noise diminution index is given as

$$i_{nr}(h_s) \triangleq \frac{\sigma_w^2}{E\{[h_{sw} w(p)]^2\}} \quad (15)$$

Then, the maximization of the cost function given by (16) is used to obtain the optimal value of α –

$$J(\alpha) \triangleq \frac{i_{nr}(h_{sw})}{i_{nr}(h_{ow})} - \beta \frac{i_{sd}(g_{sw})}{i_{sd}(g_{ow})} \quad (16)$$

Where the value of β decides the relative significance between signal retention and noise diminution, less amount of signal distortion and noise removal also result in an immense value of β. Hence obtain a good balance between them β is set to 0.7. Each patch from a patch cluster is processed through a suboptimal Wiener filter, and its denoised version is obtained. Then the denoised cluster is further obtained using the reverse PCA transform as

$$\widehat{Y_R} = U_R \widehat{P_R} \quad (17)$$

Where U_R consists of the selected eigenvectors $U_R = [u_{y1}, u_{y1}, \ldots, u_{yR}]$, $\widehat{P_R}$ indicates the estimate of corresponding signal-dominant dimensions P_R. Then all the estimated patches are stacked together and projected into the estimated image.

4. Results and Discussion

This section practically validates the adaptive variation approach for image denoising when applied to the dataset imagery detailed in the following subsections.

4.1. Experimental Platform

The implementation of the image denoising algorithm and its further performance evaluation is carried out on an experimental platform detailed in Table I.

Table 1. Details of the experimental setup

Setup item	Details
Software	MATLAB R2022a
Processor	11th Gen Intel(R) Core (TM) i5-1135G7 @ 2.40 GHz
RAM	8 GB

4.2. Dataset Imagery

Four grayscale images of dimensions 256 × 256 pixels are used for the experimentation. These dataset images named Rhinoceros, Crow, Building, and Elephant are obtained from the UC-Berkeley dataset [31].

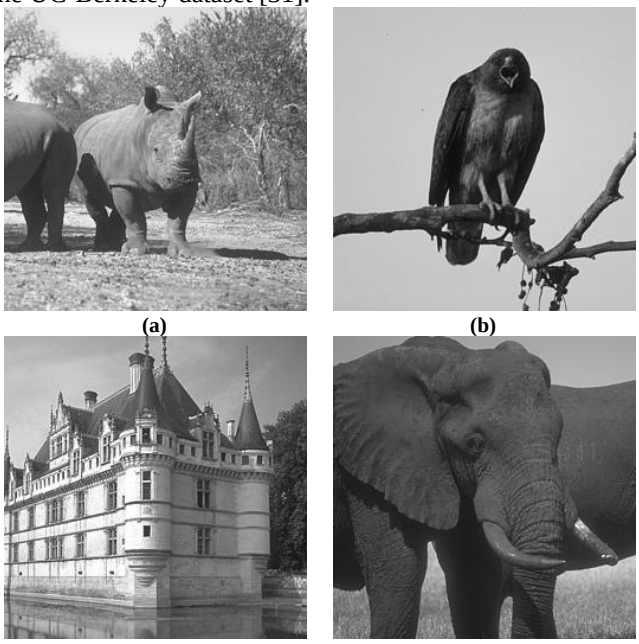

(a) (b) (c) (d)

Fig. 2 Dataset Imagery: (a) Rhinoceros, (b) Crow, (c) Building, (d) Elephant

4.3. Results

To demonstrate the performance of the various adaptive approach for image denoising, the original dataset imagery, which is free from noise, is made noisy using four noise models, correspondingly speckle, salt & pepper, Gaussian, and Poisson. The noise is added with the default parameter value in MATLAB.

The noisy images and the resultant denoised images obtained using the various adaptive approach corresponding to the four dataset images are displayed in Figures- 3, 4, 5, and 6. To quantify the performance of image denoising, the denoised images are compared to the original noise-free images, and the evaluation metrics [32], namely PSNR, SSIM, and FSIM, are computed. The obtained values of the evaluation metrics and the execution time for image denoising corresponding to four dataset images are shown in Table 2.

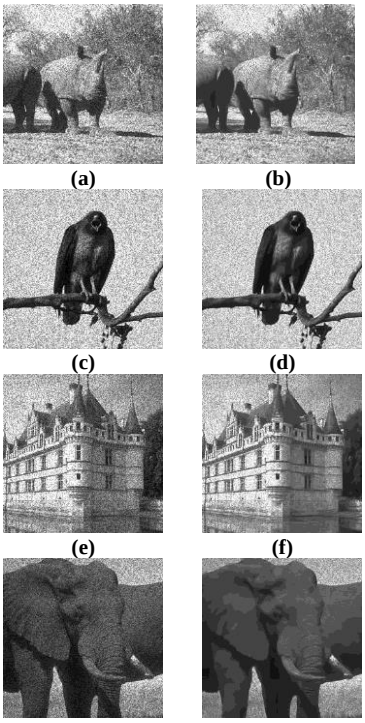

Fig. 3 Experimentation for Speckle Denoising: (a) Noisy Rhinoceros, (b) Denoised Rhinoceros, (c) Noisy Crow, (d) Denoised Crow, (e) Noisy Building, (f) Denoised Building, (g) Noisy Elephant, (h) Denoised Elephant

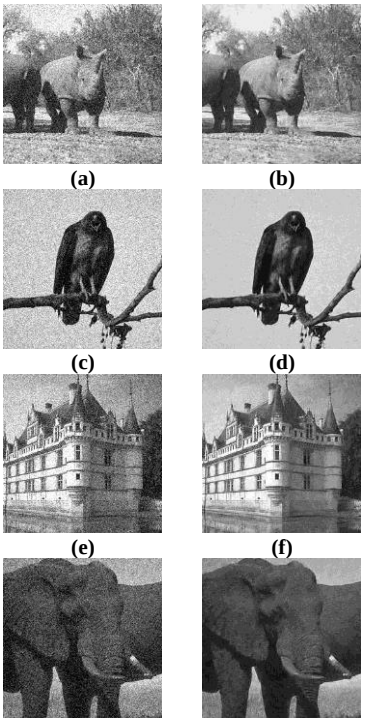

Fig. 5 Experimentation for Gaussian Denoising: (a) Noisy Rhinoceros, (b) Denoised Rhinoceros, (c) Noisy Crow, (d) Denoised Crow, (e) Noisy Building, (f) Denoised Building, (g) Noisy Elephant, (h) Denoised Elephant

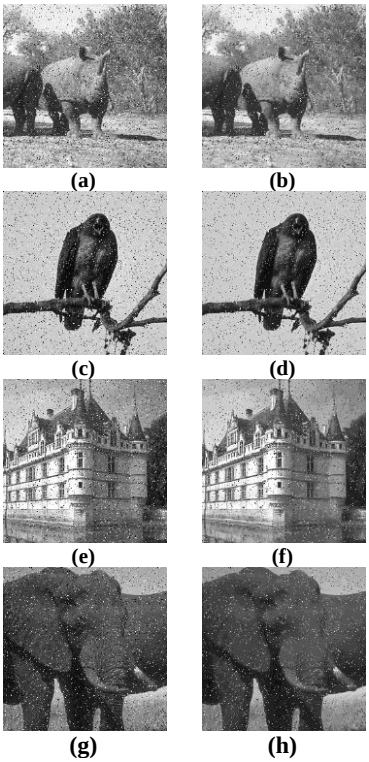

Fig. 4 Experimentation for Salt & Pepper Denoising: (a) Noisy Rhinoceros, (b) Denoised Rhinoceros, (c) Noisy Crow, (d) Denoised Crow, (e) Noisy Building, (f) Denoised Building, (g) Noisy Elephant, (h) Denoised Elephant

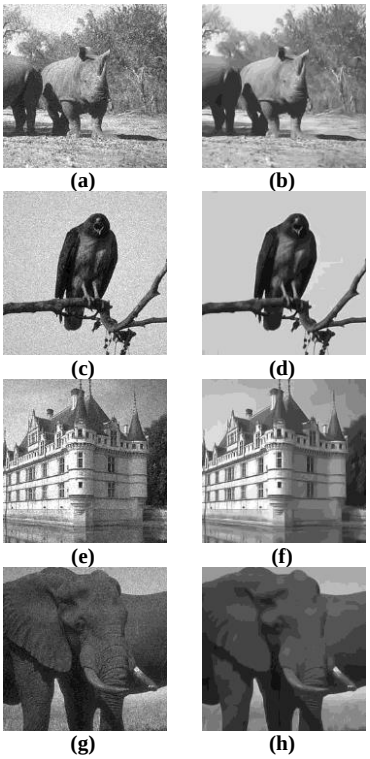

Fig. 6 Experimentation for Poisson Denoising: (a) Noisy Rhinoceros, (b) Denoised Rhinoceros, (c) Noisy Crow, (d) Denoised Crow, (e) Noisy Building, (f) Denoised Building, (g) Noisy Elephant, (h) Denoised Elephant

Table 2. Measurement of performance metrics: PSNR, SSIM, FSIM, and execution time.

Dataset Imagery	Noise Type	PSNR	SSIM	FSIM	Time (s)
Rhinoceros	Speckle	20.4024	0.5745	0.8289	116.3152
	Salt & Pepper	20.4262	0.5735	0.8597	106.8914
	Gaussian	24.7775	0.7198	0.8746	96.5399
	Poisson	27.0436	0.7831	0.8741	46.1151
Crow	Speckle	18.9186	0.3310	0.5419	106.6050
	Salt & Pepper	19.6383	0.4207	0.7834	87.4344
	Gaussian	28.6109	0.6597	0.8073	80.1020
	Poisson	33.8712	0.9477	0.9385	37.3250
Building	Speckle	21.1825	0.5838	0.8033	111.0295
	Salt & Pepper	20.7864	0.5708	0.8623	113.7823
	Gaussian	25.6806	0.7034	0.8852	97.2190
	Poisson	29.2199	0.8662	0.8998	50.2314
Elephant	Speckle	20.4049	0.5718	0.8261	433.1694
	Salt & Pepper	20.2517	0.5606	0.8535	425.7501
	Gaussian	24.7805	0.7121	0.8750	388.7226
	Poisson	27.0404	0.7827	0.8728	162.5742

Fig. 7 Comparative analysis of variation adaptive denoising approach against speckle, salt & pepper, Gaussian, and Poisson noise models considering the measurements of (a) PSNR, (b) SSIM, (c) FSIM, and (d) the execution time.

4.4. Quantitative Analysis

In order to judge the suitability of the various adaptive image denoising approach against the four noise models using the dataset imagery, it is necessary to analyze the quantified evaluation metric values. SSIM and FSIM give structural information, whereas PSNR gives information about the image reconstruction quality of the algorithm.

A graphical plot of obtained PSNR values, as shown in Figure 7(a), will be helpful here. The desired value of PSNR is always a maximum indicating the retention of signal information despite the corruption caused by noise. From the graphical plot, it is clear that the adaptive variation approach is more suitable for reducing the Poisson noise. There is also a considerable reduction in Gaussian noise in the concerned image. Handling the speckle and salt & pepper noise using the discussed methodology is inefficient. However, still, it is successful in achieving higher PSNR in speckle noise reduction for Elephant images than in the case of salt & pepper noise.

The quantification of image quality degradations in terms of perceptual metric SSIM is graphically plotted in Figure 7(b). The desired structural similarity of the denoised image with the original image is always as maximum as possible. From this plot also, it is clear that the variation adaptive approach best suits to reduce the Poisson noise. Next to this, it is also efficient to reduce Gaussian noise in an image to a considerable level. The discussed methodology's performance is inconsistent while handling the speckle and salt & pepper noise. It seems dependent on image information variation trends in the spatial plane. In the case of the Elephant image dataset, speckle noise reduction achieves a higher SSIM index than in the Gaussian and salt & pepper noise reduction.

The feature similarity of denoised images with their original counterparts measured in terms of FSIM values is plotted in Figure 7(c). The efficiency of the image-denoising algorithm also greatly depends on this metric computation. As higher the FSIM values, the more efficient the denoising algorithm is. Poisson noise reduction has achieved the highest FSIM values in this plot. The performances in the Gaussian and salt & pepper noise reduction cases are respectively very close to Poisson denoising. Comparatively, the speckle denoising fails to retain the resulting images' feature information.

Finally, a comparison of time taken for image denoising is plotted in Figure 7(d). Despite the same computational complexity of the algorithm when applied to different images corrupted by different noise types, it is found that Poisson noise reduction is achieved in the least execution time. Next, the Gaussian denoising is faster than the other two. Speckle and salt & pepper denoising using the adaptive variation approach are found to be computationally inefficient.

5. Conclusion and Future Scope

In this paper, we have validated the effectiveness of a popular image denoising approach, where the suboptimal Wiener filter operation follows an adaptive image patch clustering in the PCA domain. The experimentation is conducted on grayscale images corrupted by four different noise types: speckle, salt & pepper, Gaussian, and Poisson. The efficiency of image denoising is quantified in terms of PSNR, SSIM, FSIM, and denoising time. When the results are compared, it is observed that the method is best at reducing Poisson noise and better at reducing Gaussian noise when quality metrics and execution time are considered. The adaptive variation approach is unsuitable for efficiently handling the speckle and salt & pepper noise. The development of a more sophisticated image-denoising method that can efficiently deal with various noise models is planned for future work.

References

[1] Jiří Borovec, Jan Kybic, Ignacio Arganda-Carreras, Dmitry V. Sorokin, Gloria Bueno, Alexander V. Khvostikov, Spyridon Bakas, Eric, I-Chao Chang, Stefan Heldmann, Kimmo Kartasalo, Leena Latonen, Johannes Lotz, Michelle Noga, Sarthak Pati, Kumaradevan Punithakumar, Pekka Ruusuvuori, Andrzej Skalski, Nazanin Tahmasebi, Masi Valkonen, Ludovic Venet, Yizhe Wang, Nick Weiss, Marek Wodzinski, Yu Xiang, Yan Xu, Yan Yan, Paul Yushkevich, Shengyu Zhao, and Arrate Muñoz-Barrutia, “ANHIR: Automatic Non-Rigid Histological Image Registration Challenge,” *IEEE Transactions on Medical Imaging*, vol. 39, no. 10, pp. 3042–3052, 2020. Crossref, http://doi.org/10.1109/TMI.2020.2986331

[2] M. Li, Y. Chen, Z. Ji, K. Xie, S. Yuan, Q. Chen, and S. Li, "Image Projection Network: 3D to 2D Image Segmentation in Octa Images," *IEEE Transactions on Medical Imaging*, vol. 39, no. 11, pp. 3343–3354, 2020. Crossref, http://doi.org/10.1109/TMI.2020.2992244

[3] Y. Pei, Y. Huang, Q. Zou, X. Zhang, and S. Wang, "Effects of Image Degradation and Degradation Removal to CNN-Based Image Classification," *IEEE Transactions on Pattern Analysis and Machine Intelligence*, vol. 43, no. 4, pp. 1239–1253, 2021. Crossref, http://doi.org/10.1109/TPAMI.2019.2950923

[4] P. K. Mishro, S. Agrawal, R. Panda, and A. Abraham, "A Survey on State of-the-Art Denoising Techniques for Brain Magnetic Resonance Images," *IEEE Reviews in Biomedical Engineering*, vol. 15, pp. 184–199, 2022. Crossref, http://doi.org/10.1109/RBME.2021.3055556

[5] M. H. Alkinani and M. R. El-Sakka, "Patch-Based Models and Algorithms for Image Denoising: A Comparative Review Between Patch-Based Images Denoising Methods for Additive Noise Reduction," *EURASIP Journal on Image and Video Processing*, vol. 58, pp. 1–27, 2017. Crossref, https://doi.org/10.1186/s13640-017-0203-4

[6] K.Manivel, and Dr. R.Samson Ravindran, "A Comparative Study of Impulse Noise Reduction in Digital Images for Classical and Fuzzy Filters," *International Journal of Engineering Trends and Technology*, vol. 4, no. 10, pp. 4584-4589, 2013.

[7] Y. Vishnu Tej, M. James Stephen, PVGD. Prasad Reddy, and Praveen Choppala, "A Novel Methodology for Denoising Impulse Noise in Satellite Images through Isolated Vector Median Filter with k-means Clustering," *International Journal of Engineering Trends and Technology*, vol. 70, no. 8, pp. 272-283, 2022. Crossref, https://doi.org/10.14445/22315381/IJETT-V70I8P229

[8] R. James, A. M. Jolly, C. Anjali, and D. Michael, "Image Denoising using Adaptive PCA and SVD," in 2015 *Fifth International Conference on Advances in Computing and Communications (ICACC)*, pp. 383–386, 2015. Crossref, https://doi.org/10.1109/ICACC.2015.82.

[9] K. Dabov, A. Foi, V. Katkovnik, and K. Egiazarian, "Image Denoising with Block-Matching and 3D Filtering," in *Image Processing: Algorithms and Systems, Neural Networks, and Machine Learning*, 2006. Crossref, https://doi.org/10.1117/12.643267

[10] A. A. Yahya, J. Tan, B. Su, M. Hu, Y. Wang, K. Liu, and A. N. Hadi, "BM3D Image Denoising Algorithm Based on an Adaptive Filtering," *Multimedia Tools and Applications, Springer*, vol. 79, pp. 20391–20427, 2020. Crossref, https://doi.org/10.1007/s11042-020-08815-8

[11] J. Gao and Q. Wang, "BM3D Image Denoising Algorithm Based on K-Means Clustering," in *Advanced Graphic Communications and Media Technologies*, vol. 417, pp. 265-272, 2016. Crossref, https://doi.org/10.1007/978-981-10-3530-2_33

[12] L. Zhang, W. Dong, D. Zhang, and G. Shi, "Two-Stage Image Denoising by Principal Component Analysis with Local Pixel Grouping," *Pattern Recognition*, vol. 43, no. 4, pp. 1531–1549, 2010. Crossref, https://doi.org/10.1016/j.patcog.2009.09.023

[13] S. Routray, A. K. Ray, and C. Mishra, "An Efficient Image Denoising Method Based on Principal Component Analysis with Learned Patch Groups," *Signal, Image and Video Processing, Springer*, vol. 13, pp. 1405–1412, 2019. Crossref, https://doi.org/10.1007/s11760-019-01489-2

[14] F. Jing, H. Shaohai, and M. Xiaole, "SAR Image De-Noising Via Groupingbased PCA and Guided Filter," *Journal of Systems Engineering and Electronics*, vol. 32, no. 1, pp. 81–91, 2021. Crossref, https://doi.org/10.23919/JSEE.2021.000009

[15] D. Muresan and T. Parks, "Adaptive Principal Components and Image Denoising," in *Proceedings 2003 International Conference on Image Processing (Cat. No. 03CH37429)*, vol. 1, pp. I–101, 2003. Crossref, https://doi.org/10.1109/ICIP.2003.1246908

[16] L. Xu, J. Li, Y. Shu, and J. Peng, "SAR Image Denoising Via Clusteringbased Principal Component Analysis," *IEEE Transactions on Geoscience and Remote Sensing*, vol. 52, no. 11, pp. 6858–6869, 2014. Crossref, https://doi.org/10.1109/TGRS.2014.2304298

[17] Y. Lin, R. Hardie, and K. Barner, "Subspace Partition Weighted Sum Filters for Image Restoration," *IEEE Signal Processing Letters*, vol. 12, no. 9, pp. 613–616, 2005. Crossref, https://doi.org/10.1109/LSP.2005.853052

[18] P. Chatterjee and P. Milanfar, "Patch-Based Near-Optimal Image Denoising," *IEEE Transactions on Image Processing*, vol. 21, no. 4, pp. 1635–1649, 2012. Crossref, https://doi.org/10.1109/TIP.2011.2172799

[19] S. Suresh, S. Lal, C. Chen, and T. Celik, "Multispectral Satellite Image Denoising Via Adaptive Cuckoo Search-Based Wiener Filter," *IEEE Transactions on Geoscience and Remote Sensing*, vol. 56, no. 8, pp. 4334–4345, 2018. Crossref, https://doi.org/10.1109/TGRS.2018.2815281

[20] Leelavathi H P and Dr. J Prakash, "Effective Speckle Noise Removal of SAR Image Based on Combination of Modified PCA and HMF with Enhancement," *International Journal of Engineering Trends and Technology*, vol. 61, no. 3, pp. 171-177, 2018. Crossref, https://doi.org/10.14445/22315381/IJETT-V61P228

[21] P. Chatterjee and P. Milanfar, "Is Denoising Dead?" *IEEE Transactions on Image Processing*, vol. 19, no. 4, pp. 895–911, 2010. Crossref, https://doi.org/10.1109/TIP.2009.2037087

[22] P. Chatterjee and P. Milanfar, "Patch-Based Near-Optimal Image Denoising," *IEEE Transactions on Image Processing*, vol. 21, no. 4, pp. 1635–1649, 2012. Crossref, https://doi.org/10.1109/TIP.2011.2172799

[23] M. Cao, S. Li, R. Wang, and N. Li, "Interferometric Phase Denoising by Median Patch-Based Locally Optimal Wiener Filter," *IEEE Geoscience and Remote Sensing Letters*, vol. 12, no. 8, pp. 1730–1734, 2015. Crossref, https://doi.org/10.1109/LGRS.2015.2422788

[24] Rabiya Banu A, and Kannan R, "Quantitative and Qualitative Analysis for Lung Nodule Segmentation," *SSRG International Journal of Electronics and Communication Engineering*, vol. 6, no. 5, pp. 16-21, 2019. Crossref, https://doi.org/10.14445/23488549/IJECE-V6I5P104

[25] R. C. Gonzalez and R. E. Woods, "*Digital Image Processing*," 3rd Ed., UpperSaddle River, NJ: Prentice Hall, 2008.

[26] A. K. Boyat and B. K. Joshi, "A Review Paper: Noise Models in Digital Image Processing," ArXiv, vol. abs/1505.03489, 2015. Crossref, https://doi.org/10.48550/arXiv.1505.03489

[27] J. Bigot, C. Deledalle, and D. F'eral, "Generalized Sure for Optimal Shrinkage of Singular Values in Low-Rank Matrix Denoising," *Journal of Machine Learning Research*, vol. 18, no. 137, pp. 1–50, 2017.

[28] J. Lerga, M. Vrankic, and V. Sucic, "A Signal Denoising Method Based on the Improved ICI Rule," *IEEE Signal Processing Letters*, vol. 15, pp. 601–604, 2008. Crossref, https://doi.org/10.1109/LSP.2008.2001817.

[29] L. Zhang, W. Dong, D. Zhang, and G. Shi, "Two-Stage Image Denoising by Principal Component Analysis with Local Pixel Grouping," *Pattern Recognition*, vol. 43, no. 4, pp. 1531–1549, 2010. Crossref, https://doi.org/10.1016/j.patcog.2009.09.023

[30] J. Chen, J. Benesty, Y. Huang, and S. Doclo, "New Insights Into the Noise Reduction Wiener Filter," *IEEE Transactions on Audio, Speech, and Language Processing*, vol. 14, no. 4, pp. 1218–1234, 2006. Crossref, https://doi.org/10.1109/TSA.2005.860851

[31] 2021. [Online]. Available: https://www2.eecs.berkeley.edu/Research/Projects/CS/vision/bsds/

[32] U. Sara, M. Akter, and M. S. Uddin, "Image Quality Assessment Through FSIM, SSIM, MSE and PSNR—A Comparative Study," *Journal of Computer and Communications*, vol. 7, pp. 8–18, 2019. Crossref, https://doi.org/10.4236/jcc.2019.73002

[33] K. Ote, F. Hashimoto, A. Kakimoto, T. Isobe, T. Inubushi, R. Ota, A. Tokui, A. Saito, T. Moriya, T. Omura, E. Yoshikawa, A. Teramoto, and Y. Ouchi, "Kinetics-Induced Block Matching and 5-D Transform Domain Filtering for Dynamic Pet Image Denoising," *IEEE Transactions on Radiation and Plasma Medical Sciences*, vol. 4, no. 6, pp. 720–728, 2020. Crossref, https://doi.org/10.1109/TRPMS.2020.3000221